Journal of The Electrochemical Society, **156** (1) B167-B173 (2009)
0013-4651/2008/156(1)/B167/7/$23.00 © The Electrochemical Society

Kinetic Study of the Hydrogen Electrode Reaction on Bi-Modified Platinum

Paola M. Quaino, María R. Gennero de Chialvo, and Abel C. Chialvo[z]

Programa de Electroquímica Aplicada e Ingeniería Electroquímica (PRELINE), Facultad de Ingeniería Química, Universidad Nacional del Litoral, 3000 Santa Fe, Argentina

The present work deals with a kinetic study of the hydrogen electrode reaction (HER) on a platinum electrode modified by bismuth adatoms in both the cathodic and anodic range of overpotentials. Kinetic expressions previously derived for the Volmer–Heyrovsky–Tafel mechanism were modified in order to take into account the influence of bismuth. Thus, a modification of the adsorption energy of the reaction intermediate, described through the variation of the Frumkin interaction parameter, and a possible effect of inhibition on the active sites were included in the kinetic expressions. On this basis, the experimental results obtained in the overpotentials range $-0.20 < \eta/V < 0.40$ were successfully correlated through the variation of only four adjustable parameters, whose dependence on the bismuth surface coverage was evaluated and discussed.
 [DOI: 10.1149/1.3021409]

Manuscript submitted July 21, 2008; revised manuscript received October 13, 2008. Published November 19, 2008.

The hydrogen electrode reaction (HER) is of fundamental importance in electrochemistry and has been the subject of numerous investigations. It is the anodic reaction in the most common type of low-temperature fuel cell as well as the cathodic reaction in water electrolysis for the production of hydrogen. Nevertheless, several kinetic aspects still remain uncertain. The kinetics of the HER has been mainly studied on the basis of the experimental current–potential curves obtained in the potential region corresponding to the hydrogen evolution reaction (*her*) and interpreted through the Volmer–Heyrovsky–Tafel mechanism.[1-10] It has been considered that this reaction takes place under activated control conditions, which implies that the concentration of the molecular hydrogen at the electrode surface is equal to that in the bulk solution. A marked variation of the surface coverage of the adsorbed reaction intermediate on overpotential was also found. However, for the formation of hydrogen bubbles, the solution surrounding the electrode should be oversaturated. Then, the surface concentration should be greater than that of the bulk, originating a flow of molecular hydrogen from the electrode surface. This excess surface hydrogen concentration, which can be described through the hydrogen supersaturation α, can reach significantly high values ($\alpha > 100$) and have a strong effect on the experimental current–potential curves.[11] Therefore, the kinetic study of the *her* requires well-defined diffusion conditions and theoretical expressions that describe appropriately the electrode processes.

The hydrogen oxidation reaction (*hor*), which must involve the same kinetic elementary steps as the *her*, has been historically considered as taking place in one path involving the transference of two electrons under mixed-control conditions, although with a predominance of the diffusion contribution.[12-14] Only recently have kinetic studies involving the elementary steps been developed.[15-17] It has also been found that the reaction takes place with low values of the surface coverage of the adsorbed reaction intermediate.[18-21] Besides, the theoretical treatment of the *hor* on platinum under steady-state conditions has demonstrated that the reaction can present a clear prevalence of the Tafel–Volmer route at low overpotentials, which is replaced by the Heyrovsky–Volmer route as the potential is increased.[18-20] Consequently, it has been predicted that the current–potential curve can exhibit two current plateaus, indicating the transition between those routes. In the case of platinum, for the observation of this phenomenon the thickness of the diffusion layer must be less than those reached with a rotating disk electrode (RDE), although it is clearly shown on microelectrodes.[20,21]

Another important aspect in the description of the reaction kinetics of the hydrogen electrode is related to the nature of the adsorbed hydrogen involved as the reaction intermediate. For the platinum electrode, the existence of two types of adatoms denominated respectively, H_{UPD} (underpotentially deposited) and H_{OPD} (overpotentially deposited) is well known.[8,9] The H_{UPD} is that which defines the characteristic peaks in the profile resulting from the application of a potentiodynamic sweep. It was found from spectroscopic studies that the reaction intermediate is a hydrogen atom adsorbed "on top," different from that shown voltammetrically.[22-24] Consequently, the study of the influence on the kinetics of the HER of the adsorption of metallic atoms, covering surface sites corresponding to the H_{UPD}, can bring evidences about the behavior and nature of the reaction intermediate. Bismuth was used in the present case, because although its effect has been analyzed previously,[25-28] the availability of new tools for the evaluation of the reaction in the whole range of overpotentials, as well as the experimental conditions used in those studies, makes it worthwhile to carry out this study in order to improve the present knowledge about this subject and give insight on the behavior of the reaction intermediate. The pioneer works in this subject for the *her*[25,26] and *hor*[28] considered that the blockage of the adsorption sites of the reaction intermediate is the main reason for the decrease in the reaction rate. A more recent study on the *hor*[27] concluded that, besides blockage, adsorbed bismuth Bi_{ad} alters the electronic properties of the adjacent Pt sites, but the study did not develop any kinetic mechanism for the interpretation of the results.

In this context, the present work deals with the study of the kinetics of the HER on a smooth polycrystalline platinum electrode covered with different amounts of bismuth atoms in a wide range of overpotentials ($-0.20 < \eta/V < 0.40$), with the purpose of bringing new evidence to enlighten the behavior and nature of the reaction intermediate and the influence of adsorbed bismuth.

Experimental

Cell description.— The experimental determinations were carried out in three-electrode Pyrex glass cells. Two different cells were used, one for the Bi adsorption and another for the voltammetric characterization and the kinetic measurements under rotating conditions. Large-area platinum counter electrodes and hydrogen-bubble reference electrodes immersed in the electrolyte solution were used in both cells. Special attention was paid to the purity of the electrolyte solutions, which was verified by essays of adsorption–oxidation before each experimental run.

Preparation of Pt/Bi_{ad} electrodes.— The irreversible adsorption of bismuth on a clean platinum electrode was carried out potentiostatically in a $5\ 10^{-4}$ M $Bi_2(SO_4)_3$ solution prepared from Bi_2O_3 dissolved in 0.5 M H_2SO_4 solution. The adsorption potential E_{ad} was fixed to −0.02 V and the time of application t_{ad} was varied in order to obtain different values of the Bi coverage ($30s \leqslant t_{ad} \leqslant 600s$). The electrodes were then removed from the cell at closed circuit and immediately washed in order to avoid adsorption by

[z] E-mail: achialvo@fiq.unl.edu.ar

contact. At $E_{ad} < -0.07$ V, the massive deposition of Bi is produced. The Pt/Bi_{ad} electrode was never subjected to potentials greater than 0.60 V to avoid the oxidation or dissolution of bismuth.

Treatment of Pt electrodes.— The polycrystalline platinum electrodes subjected to a bismuth adsorption process cannot be recovered through conventional pretreatments such as anodic electrodesorption, as the Bi_{ad} cannot be eliminated from the electrode surface even after a large number of desorption cycles. Therefore, a procedure was developed in order to obtain Pt electrodes free from Bi_{ad}, with a reproducible voltammetric shape independent of their previous history. This experimental treatment consisted of the following steps: (*i*) polishing with emery paper 2500, (*ii*) polishing with alumina powder 0.5 μm, (*iii*) growth of a PtO_2 layer in acid solution through the application of periodic potential signals of high amplitudes and frequencies,[29] and (*iv*) removal of this oxide film by polishing as in (*i*) and (*ii*).

Voltammetric characterization.— The working electrodes were subjected to cyclic voltammetry (CV) in a 0.5 M H_2SO_4 solution free from Bi^{3+} ions at a sweep rate of 0.025 V s^{-1}. The aim of these voltammetric runs were: (*i*) characterization of Pt electrode, (*ii*) verification of the purity of the electrolyte solutions, and (*iii*) quantification of the amount of Bi_{ad}. In the first case, the potentiodynamic sweep was applied between 0.05 and 1.5 V in order to obtain the corresponding voltammogram. The verification of the purity of the electrolyte solution was made through the application of two consecutive steps of potentiostatic adsorption on a rotating Pt disk at 8100 rpm under nitrogen bubbling at −0.05 V during 5 min and 0.0 V during another 5 min, respectively. Immediately after the adsorption and without interrupting the electric circuit, a potentiodynamic sweep in the anodic direction was applied, followed by repetitive cycles. The purity of the solution is determined by the absence of peaks or electro-oxidation processes different from those characteristic of the Pt electrode or the invariance of the current peaks related to the H_{UPD} electrosorption. Finally, for the evaluation of the amount of Bi_{ad}, a potentiodynamic sweep was recorded in the range 0.05–0.425 V, and the voltammetric charge in the H_{UPD} region was calculated.

Kinetic measurements.— The evaluation of the $j(\eta)$ experimental dependence for the HER on Pt/Bi_{ad} modified electrodes was made with a RDE operated at 8100 rpm in 0.50 M H_2SO_4 (free of Bi^{+3} ions in solution) at 30°C and with continuous hydrogen bubbling (99.999% purity) to ensure the saturation conditions at a pressure of 1 atm. One of the most important requirements that must be fulfilled to study the HER is that the reversible potential must be defined and maintained stable with time. In the specific case of the Pt/Bi_{ad} electrode, if the solution is perfectly pure and there is no other type of polluting agent in the system, the electrodes quickly reach the reversible potential. Starting from this value, two different experimental methods were applied with identical results. One consisted of a potential pulse to the desired overpotential, which was maintained for 30 s. During this period, lectures of the current value were made every 2 s, and the mean value of the last 20 s was assigned to this overpotential. The other consisted of the application of a slow potentiodynamic sweep at 0.008 V s^{-1}, so the time needed for each run was small enough to avoid any type of contamination of the electrode surface. The methodology for the generation and acquisition of the experimental data was described previously.[19,30]

Results

Electrode characterization.— Previous to the bismuth electroadsorption, the platinum electrode was characterized by CV between 0.05 and 1.50 V in 0.5 M H_2SO_4 solution to verify the appropriate reproducible initial state of the platinum substrate (Fig. 1, line a). The voltammetric behavior of the Pt/Bi_{ad} was almost independent of the adsorption potential E_{ad}, although the amount of Bi_{ad} depends strongly upon time t_{ad}. Figure 1 (line b) is the profile obtained after

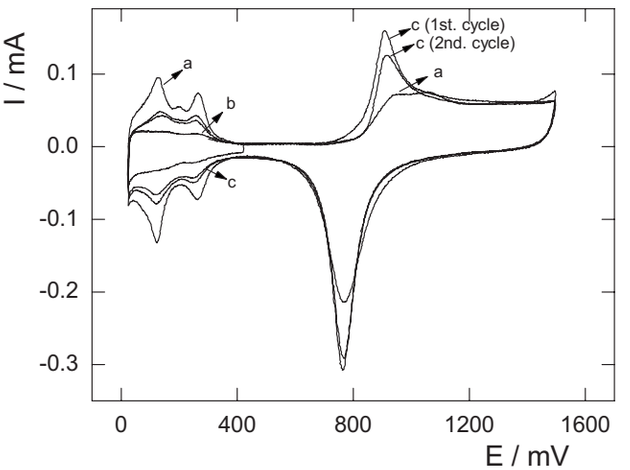

Figure 1. Cyclic voltammograms: (a) before Bi adsorption, (b) after Bi adsorption $\theta_{Bi} = 0.73$, and (c) first and second extended cycle after (b). 0.50 M H_2SO_4; 0.025 V s^{-1}; 30 C.

Bi adsorption at $E_{ad} = -0.020$ V during 30 s, recorded between 0.05 and 0.425 V for the evaluation of the bismuth surface coverage. Finally, Fig. 1 (line c) is the response obtained after line b when the potentiodynamic sweep is extended to 1.5 V (first and second cycle). This profile shows a current peak at 0.90 V during the anodic sweep and a significant increase of the cathodic charge corresponding to the electroreduction of O_{ad}. Another important aspect is that the repetitive cycling between 0.05 and 0.425 V does not change the voltammetric profile, whereas the potentiodynamic sweep between 0.05 and 1.5 V produces a continuous decrease cycle by cycle of the anodic peak located at 0.90 V as well as an increase of the peaks corresponding to the adsorbed hydrogen (H_{UPD}), indicating a loss of bismuth. If the upper potential is held below 0.6 V, the voltammetric profile is invariant, and therefore the Bi_{ad} layer can be considered stable. Consequently, an apparent surface coverage of Bi_{ad} (θ_{Bi}) was determined on the basis of the difference in the voltammetric charge in 0.5 M H_2SO_4 solution, between 0.05 and 0.425 V, before and after the Bi adsorption.[31,32] The corresponding expression is

$$\theta_{Bi} = \frac{(Q^{Pt}_{H_{UPD}} - Q^{Pt/Bi_{ad}}_{H_{UPD}})}{Q^{Pt}_{H_{UPD}}} \quad [1]$$

where $Q^{Pt}_{H_{UPD}}$ is the anodic voltammetric charge in the H_{UPD} region on the Pt electrode and $Q^{Pt/Bi_{ad}}_{H_{UPD}}$ is the anodic voltammetric charge in the same region on the Pt/Bi_{ad} electrode.

Experimental dependence $j(\eta)$.— The variation of current density on overpotential for the HER was evaluated in the range ($-0.20 \leqslant \eta/V \leqslant 0.40$) at a rotation rate of 8100 rpm for 5 values of the bismuth surface coverage ($\theta_{Bi} = 0.07$, 0.31, 0.54, 0.635, and 0.73). In order to illustrate in detail the different regions, Fig. 2 and 3 show the response corresponding to the range of cathodic and anodic overpotentials, respectively, where symbols indicate the experimental values. A decrease of the electrocatalytic activity can be observed for the *her* ($-0.20 \leqslant \eta/V \leqslant 0.0$) with the increment of the bismuth surface coverage. For the *hor* ($0.0 \leqslant \eta/V \leqslant 0.40$) no effect due to the presence of Bi adatoms on the experimental value of the maximum current density (j_{max}) is observed.

Kinetic description.— The kinetic description of the HER requires, in this case, the incorporation of the interaction effect of the bismuth surface coverage on the adsorption of the reaction intermediate as well as a possible effect of inhibition of the OPD active sites. The first aspect can be taken into account through the evaluation of a Frumkin interaction parameter u for each θ_{Bi} value and

then, starting from the correlation of the experimental results, the function $u(\theta_{Bi})$ can be obtained. However, it is accepted from kinetic[8,10,19] and spectroscopic[22-24,33] evidences that the reaction intermediate involved in the HER is the adsorbed hydrogen of the type H_{OPD}. However, it is reasonable to consider, in principle, that the presence of Bi_{ad} occupying H_{UPD} sites can produce a certain degree of inhibition in the H_{OPD} adsorption. In this context, the balance of the OPD sites can be written as

$$\theta_H^{OPD} + \theta_{inh}^{OPD} + \theta_{free}^{OPD} = 1 \qquad [2]$$

where θ_H^{OPD} is the surface coverage of the reaction intermediate, θ_{inh}^{OPD} is the fraction of H_{OPD} sites inhibited due to the presence of Bi adatoms on the H_{UPD} sites, and θ_{free}^{OPD} is the unoccupied fraction of OPD sites. It is important to note the difference between θ_{Bi}, which is the fraction of H_{UPD} sites occupied by the bismuth atoms, and θ_{inh}^{OPD}. Consequently, it is expected that $\theta_{inh}^{OPD} = f(\theta_{Bi})$. Another important aspect is that a bismuth atom cannot originate an adsorption site for hydrogen.[34,35]

On this basis, the kinetic expressions for the HER, previously derived for surfaces free of metallic adatoms under the Volmer–Heyrovsky–Tafel mechanism,[30] can be rewritten as

$$j = \frac{v_V^e\left[\frac{\theta}{\theta^e}e^{\alpha_V f\eta}e^{u(\theta-\theta^e)} - \frac{(1-\theta-\theta_{inh})}{(1-\theta^e-\theta_{inh})}e^{-(1-\alpha_V)f\eta}\right] + v_H^e\left[\frac{(1-\theta-\theta_{inh})}{(1-\theta^e-\theta_{inh})}e^{\alpha_H f\eta} - \frac{\theta}{\theta^e}e^{-(1-\alpha_H)f\eta}e^{u(\theta-\theta^e)}\right]}{\left[\frac{e^{\lambda u(\theta-\theta^e)}}{F} + \frac{v_H^e}{j_L}\left(\frac{1-\theta-\theta_{inh}}{1-\theta^e-\theta_{inh}}\right)e^{\alpha_H f\eta}\right]} \qquad [3a]$$

$$j = \frac{v_T^e\left[\left(\frac{1-\theta-\theta_{inh}}{1-\theta^e-\theta_{inh}}\right)^2 e^{-\lambda u(\theta-\theta^e)} - \left(\frac{\theta}{\theta^e}\right)^2 e^{(2-\lambda)u(\theta-\theta^e)}\right] + v_H^e\left[\left(\frac{1-\theta-\theta_{inh}}{1-\theta^e-\theta_{inh}}\right)e^{\alpha_H f\eta} - \left(\frac{\theta}{\theta^e}\right)e^{-(1-\alpha_H)f\eta}e^{u(\theta-\theta^e)}\right]}{\left[\frac{e^{\lambda u(\theta-\theta^e)}}{2F} + \frac{v_H^e}{j_L}\left(\frac{1-\theta-\theta_{inh}}{1-\theta^e-\theta_{inh}}\right)e^{\alpha_H f\eta} + \frac{v_T^e}{j_L}\left(\frac{1-\theta-\theta_{inh}}{1-\theta^e-\theta_{inh}}\right)^2 e^{-\lambda u(\theta-\theta^e)}\right]} \qquad [3b]$$

$$j = \frac{v_V^e\left[\left(\frac{\theta}{\theta^e}\right)e^{\alpha_V f\eta}e^{u(\theta-\theta^e)} - \left(\frac{1-\theta-\theta_{inh}}{1-\theta^e-\theta_{inh}}\right)e^{-(1-\alpha_V)f\eta}\right] - v_T^e\left[\left(\frac{1-\theta-\theta_{inh}}{1-\theta^e-\theta_{inh}}\right)^2 e^{-\lambda u(\theta-\theta^e)} - \left(\frac{\theta}{\theta^e}\right)^2 e^{(2-\lambda)u(\theta-\theta^e)}\right]}{\left[\frac{e^{\lambda u(\theta-\theta^e)}}{2F} - \frac{v_T^e}{j_L}\left(\frac{1-\theta-\theta_{inh}}{1-\theta^e-\theta_{inh}}\right)^2 e^{-\lambda u(\theta-\theta^e)}\right]} \qquad [3c]$$

where v_i ($i = V, H, T$) is the reaction rate of the step i, α_i ($i = V, H$) is the symmetry factor of the reaction step i, and λ is the symmetry factor of adsorption and u [in room temperature (RT) units] is the energy of interaction between the adsorbed hydrogen atoms. The superscript OPD and the subscript H on θ were omitted in the equation in order to simplify the nomenclature. Superscript e indicates equilibrium and $f = F/RT$. Finally, j_L is the limiting diffusion current density of the molecular hydrogen oxidation, which is achieved when the concentration of the molecular hydrogen in the electrode surface becomes zero.

In order to evaluate the dependence $j = j(\eta, j_L, \theta^e, \theta_{inh})$, it is necessary to know the corresponding expression for $\theta = \theta(\eta, j_L, \theta^e, \theta_{inh})$, which can be obtained by reordering any of the equalities of Eq. 3. Considering the first and third term and reordering, the following expression is obtained

$$\begin{aligned}
&2v_T^e\left[e^{-\lambda u(\theta-\theta^e)}\left(\frac{1-\theta-\theta_{inh}}{1-\theta^e-\theta_{inh}}\right)^2 - e^{(2-\lambda)u(\theta-\theta^e)}\left(\frac{\theta}{\theta^e}\right)^2\right] \\
&+ \left[v_H^e e^{\alpha_H f\eta} + v_V^e e^{-(1-\alpha_V)f\eta}\right]\left(\frac{1-\theta-\theta_{inh}}{1-\theta^e-\theta_{inh}}\right) \\
&- \left[v_H^e e^{-(1-\alpha_H)f\eta} + v_V^e e^{\alpha_V f\eta}\right]e^{u(\theta-\theta^e)}\left(\frac{\theta}{\theta^e}\right) \\
&+ \frac{2Fv_T^e}{j_L}\left[v_H^e e^{-(1-\alpha_H)f\eta} - v_V^e e^{\alpha_V f\eta}\right]e^{(1-2\lambda)u(\theta-\theta^e)} \\
&\times\left(\times\frac{1-\theta-\theta_{inh}}{1-\theta^e-\theta_{inh}}\right)^2\left(\frac{\theta}{\theta^e}\right) + \frac{2Fv_T^e}{j_L}\left(\frac{1-\theta-\theta_{inh}}{1-\theta^e-\theta_{inh}}\right) \\
&\times\left[\times v_V^e e^{-2\lambda u(\theta-\theta^e)}e^{-(1-\alpha_V)f\eta}\left(\frac{1-\theta-\theta_{inh}}{1-\theta^e-\theta_{inh}}\right)^2\right. \\
&\left. - v_H^e e^{\alpha_H f\eta}e^{2(1-\lambda)u(\theta-\theta^e)}\left(\frac{\theta}{\theta^e}\right)^2\right] + \frac{2Fv_V^e v_H^e}{j_L}\left(\frac{1-\theta-\theta_{inh}}{1-\theta^e-\theta_{inh}}\right) \\
&\times\left[\times e^{-(1-\alpha_V-\alpha_H)f\eta}e^{-\lambda u(\theta-\theta^e)}\left(\frac{1-\theta-\theta_{inh}}{1-\theta^e-\theta_{inh}}\right)\right. \\
&\left. - e^{(\alpha_V+\alpha_H)f\eta}e^{(1-\lambda)u(\theta-\theta^e)}\left(\frac{\theta}{\theta^e}\right)\right] = 0
\end{aligned} \qquad [4]$$

Equation 4 is reduced to the expression obtained previously when the fraction of H_{OPD} sites inhibited by the presence of Bi_{ad} is annulled.[30]

Finally, in order to establish the variation of the surface concentration of the molecular hydrogen $c_{H_2}^s$ on overpotential, the relationship in terms of pressure $P_{H_2}^s/P_{H_2}^o$ ($\equiv c_{H_2}^s/c_{H_2}^o$) is evaluated, where the superscript o indicates the property value in the bulk solution. It can be straightforwardly determined from the following expression[18]

$$\frac{P_{H_2}^s(\eta)}{P_{H_2}^o} = 1 - \frac{j(\eta)}{j_L} \qquad [5]$$

In the cathodic region, where this relationship is $P_{H_2}^s/P_{H_2}^o > 1$, it is known as hydrogen supersaturation (α).

Evaluation of kinetic parameters.— The kinetic parameters θ^e, v_T^e, v_H^e, v_V^e, α_V, α_H, θ_{inh}, u, and λ can be evaluated through the simultaneous correlation of the experimental results $j_{exp}(\eta)$ shown in Fig. 2 and 3 (symbols) using Eq. 3 and 4 by means of the nonlinear least-squares method. Certain experimental facts make it possible to reduce the number of adjustable parameters. At first, the existence of a maximum current density (j_{max}) in the anodic region in conditions of mixed control implies that the Tafel–Volmer route prevails over the Heyrovsky–Volmer route and that $\theta(\eta) \to 0$.[18,19] Applying the condition $\eta \gg 0$ to Eq. 3c, the following expression is obtained

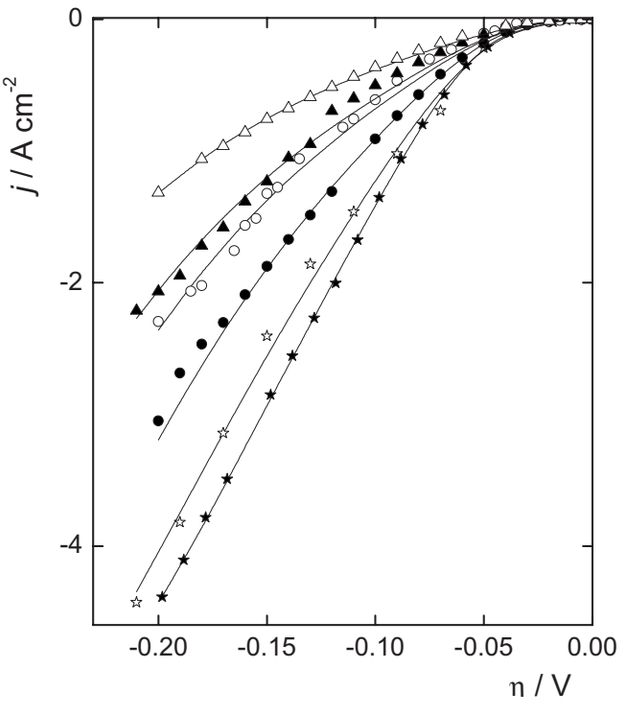

Figure 2. Experimental and simulated $j(\eta)$ dependences in the cathodic η region. ω = 8100 rpm; 30 C. θ_{Bi}: (★) 0,[30] (☆) 0.07, (●) 0.31, (○) 0.54, (▲) 0.635, and (△) 0.73.

$$\frac{1}{j_{max}} = \frac{1}{j_{max}^{kin}} + \frac{1}{j_L} \qquad [6]$$

Equation 6 expresses the mixed kinetic control, where the activated contribution corresponds to the limiting kinetic current density j_{max}^{kin},

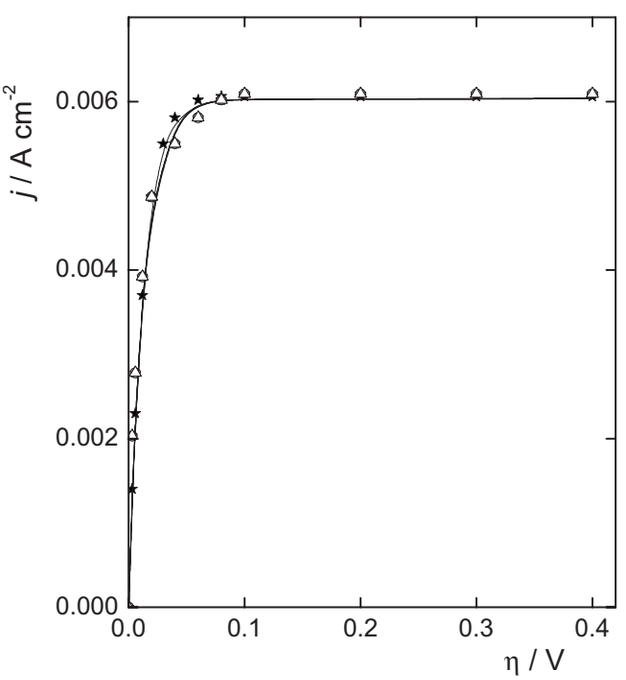

Figure 3. Experimental and simulated $j(\eta)$ dependences in the anodic η region. ω = 8100 rpm; 30 C. θ_{Bi}: (★) 0,[30] (☆) 0.07, (●) 0.31, (○) 0.54, (▲) 0.635, and (▲) 0.73.

which is originated in the Tafel step and is given by

$$j_{max}^{kin} = \frac{(1-\theta_{inh})^2 2F v_T^e e^{2\lambda u \theta^e}}{(1-\theta^e-\theta_{inh})^2} \qquad [7]$$

Equation 7 generates a relationship among the parameters $j_{max}^{kin} = j_{max}^{kin}(v_T^e, \lambda, \theta^e, \theta_{inh}, u)$, which should be considered during the correlation. The value j_{max}^{kin} = 0.235 A cm^{-2} was used, obtained from the study of the HER on a smooth Pt electrode in similar experimental conditions.[30] As the Heyrovsky step has little influence on the range of overpotentials analyzed, the values obtained previously for the equilibrium reaction rate (v_H^e = 2.07 10^{11} mol cm^{-2} s^{-1}) and the symmetry factor (α_H = 0.5) were employed. The limiting diffusion current density was determined previously (j_L = 0.00619 A cm^{-2}).[30] Finally, the Frumkin symmetry factor was fixed to λ = 0.5. Under these conditions, the number of adjustable parameters was five (v_V^e, α_V, u, θ^e, θ_{inh}). Surprisingly, the regression of the experimental dependences $j_{exp}(\eta, \theta_{Bi})$ indicated that they can be appropriately described with θ_{inh} = 0, even at high values of the bismuth surface coverage θ_{Bi}. Therefore, the final adjustable parameters were reduced to four (v_V^e, α_V, u and θ^e).

The values of the kinetic parameters obtained from the correlation of the experimental data of the HER on a Pt electrode covered with different amounts of bismuth in the whole range of overpotentials ($-0.20 \leq \eta/V \leq 0.40$) at a rotation rate of 8100 rpm are given in Table I. The simulations of the dependence $\log j(\eta)$ with these parameters for the different values of θ_{Bi} are illustrated in Fig. 4a, while Fig. 4b shows the corresponding plots of $\theta(\eta)$ and Fig. 4c the logarithm of the relationship $P_{H_2}^s(\eta)/P_{H_2}^o$. The curve corresponding to the pure platinum electrode evaluated previously was also included in each plot (dashed line).[30] It is shown in Fig. 4b and c that the dependence $\theta(\eta)$ on the overpotentials region $0.1 < \eta < 0.4$ is annulled, while the superficial hydrogen concentration is still finite and constant [$P_{H_2}^s(\eta)/P_{H_2}^o$ = 0.025]. This relationship begins to decrease again at $\eta > 0.5$ V, reaching, for example, a value of $P_{H_2}^s(\eta)/P_{H_2}^o \cong 0.0001$ for $\eta \cong 0.8$ V (not shown in the figure). This is precisely the reason why the hydrogen oxidation occurs under a mixed control in the range of overpotentials under study. In the cathodic region, the supersaturation shows a continuous increase in overpotential, reaching the value $P_{H_2}^s(\eta)/P_{H_2}^o = 100$ at $\eta \cong -0.07$ V for Pt, similar to that reported in the literature,[36] and at $\eta \cong -0.13$ V for Pt/Bi$_{ad}$ (θ_{Bi} = 0.74).

Simulations are also shown as continuous lines in Fig. 2 and 3, a good agreement is observed between the experimental data and the corresponding simulation for both *her* and *hor* directions. Finally, Fig. 5a-d shows the variation of the adjustable parameters u/RT, v_V^e, θ^e, and α_V, respectively, with the surface coverage of the adsorbed bismuth. The Frumkin interaction parameter u and the symmetry factor of the Volmer step α_V increase with θ_{Bi}. Meanwhile, the equilibrium reaction rate of the Volmer step v_V^e and the equilibrium surface coverage of the adsorbed hydrogen θ^e show a slight and nonlinear decrease as θ_{Bi} increases.

Discussion

In the present work, the dependence $j(\eta)$ for the HER was measured in a wide range of cathodic and anodic potentials on a platinum RDE modified by bismuth adatoms. These experimental dependences were interpreted by means of the Volmer–Heyrovsky–Tafel mechanism, including a Frumkin-type description of the adsorption process of the reaction intermediate H_{OPD}. The possibility of inhibition of the OPD active sites on the part of Bi_{ad} has also been considered. On this basis, starting from the theoretical expressions $j(\eta)$ and $\theta(\eta)$ and by means of a nonlinear correlation of the experimental results, the kinetic parameters that characterize the HER were determined.

Table I. Kinetic parameters for the HER at different Bi coverages obtained from the correlation of the experimental results ($-0.2 < \eta/V < 0.4$).

Kinetic parameters	Bismuth surface coverage				
	0.07	0.31	0.54	0.635	0.74
$v_T^e \times 10^7$ mol cm^{-2} s^{-1}	7.87	8.03	8.12	8.14	8.19
$v_H^e \times 10^{11}$ mol cm^{-2} s^{-1}	2.07	2.07	2.07	2.07	2.07
$v_V^e \times 10^{6a}$ mol cm^{-2} s^{-1}	1.18	6.8	4.42	3.62	2.31
$\theta^{e a}$	0.174	0.167	0.164	0.163	0.162
u/RT^a	0.35	0.38	0.41	0.425	0.44
α_V^{a}	0.56	0.575	0.59	0.60	0.615
α_H	0.5	0.5	0.5	0.5	0.5
λ	0.5	0.5	0.5	0.5	0.5

[a] Adjustable parameter.

Analysis of the dependence of kinetic parameters on θ_{Bi}.— Figure 5a shows a linear increase of the Frumkin interaction parameter u on the Bi_{ad} surface coverage, which implies an increase of the repulsive interaction between the H_{OPD} adatoms. Starting from this evidence, the following expression was found for $u(\theta_{Bi})$, in RT units

$$u(\theta_{Bi}) = 0.338 + 0.138\theta_{Bi} \quad [8]$$

The value $u(\theta_{Bi} = 0) = 0.338$ is coincident with that obtained previously for the Pt electrode, which is illustrated in Fig. 5a by the symbol ○.[30] This fact is significant, because the increment of the parameter is responsible for the decrease of the reaction rate of the *her*. In the absence of a process of inhibition of the H_{OPD} adsorption sites ($\theta_{inh} = 0$), the presence of the bismuth adatoms would only alter the adsorption properties of the OPD sites through the modification of the electronic density of states of the adjacent platinum

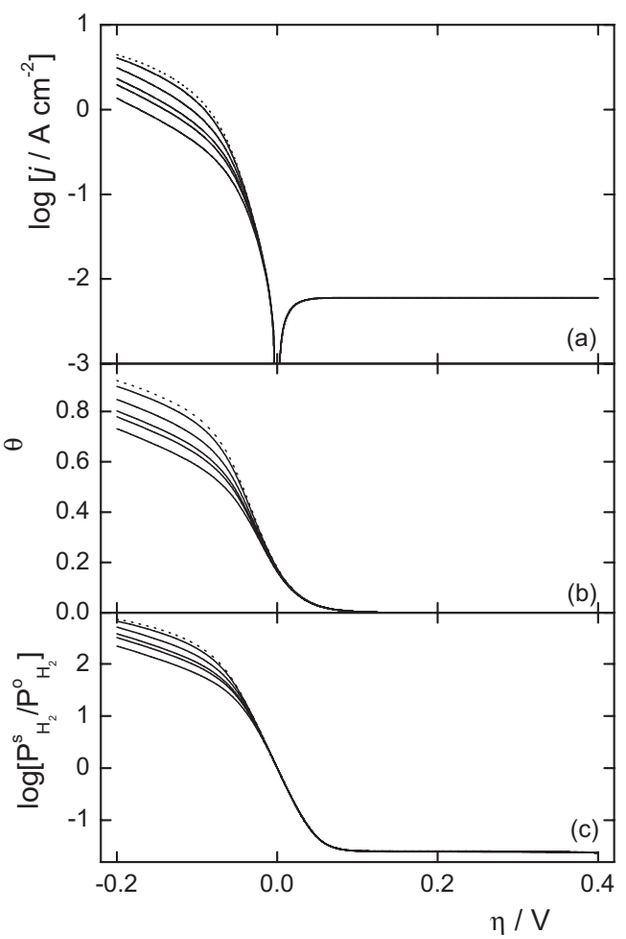

Figure 4. Simulated dependences at different Bi coverages ($0.07 \leq \theta_{Bi} \leq 0.73$) with kinetic parameters from Table I: (a) log j vs η, (b) θ vs η, and (c) log $P^s_{H_2}(\eta)/P^o_{H_2}$ vs η. Dashed lines: Pt electrode.

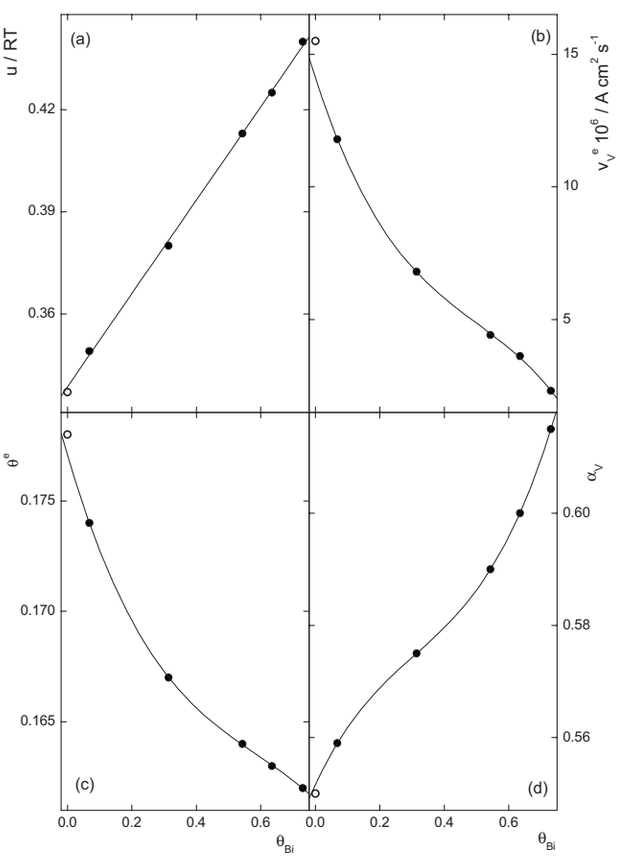

Figure 5. Variation of the kinetic parameters with θ_{Bi}; (a) u/RT, (b) v_V^e, (c) θ^e, and (d) α_V. (●) Pt electrode.

atoms.[27] This situation is reflected basically in the dependence of the interaction parameter u with θ_{Bi}. Other effects are the slight decrease of both the equilibrium reaction rate of the Volmer step v_V^e (Fig. 5b) and the equilibrium surface coverage of the reaction intermediate θ^e (Fig. 5c). In this sense, as the values of θ^e are relatively low, the average distance between the OPD hydrogen atoms is high, and therefore the effect is not quite strong.

Finally, it can be appreciated again that all these variations are self-consistent, as when these plots are extrapolated to $\theta_{Bi} = 0$, both dependences lead to those parameters values corresponding to the Pt electrode (indicated in Fig. 5a-d by the symbol ○).[30]

Comparison with previous studies.— The dependence $j(\eta,\theta_{Bi})$ corresponding to the whole domain of overpotentials of the HER shows a markedly different behavior in the anodic and cathodic regions. In the case of the *her*, a negative effect of the adsorbed bismuth on the electrocatalytic activity can be appreciated; this is coincident with previous results obtained on Pt(100) and Pt(111), which were explained through a statistical model based on the existence of three types of active sites: blocked, unaffected, and infected, but combined with a Langmuir adsorption of the reaction intermediate.[25,26] Another study in the anodic region carried out on a rotating Pt(111) disk electrode in 0.1 M $HClO_4$ solution showed a slight decrease in the maximum current density of the *hor* in the presence of Bi_{ad}, although in the case of $\omega = 900$ rpm the current plateau is almost equal to that of the Pt(111) free of bismuth.[27] The authors considered that this behavior does not correspond to a diffusion-limited current, but the origin of the observed plateau was not explained. From our point of view, this plateau corresponds to j_{max}, which is smaller than j_L and is due to the mixed kinetic control of the *hor*, according to Eq. 6. Consequently, unlike polycrystalline platinum, the hydrogen oxidation on Pt(111) shows a more pronounced effect of Bi_{ad} on the maximum current density, which in principle can be assigned to a decrease in the j_{max}^{kin} value on this type of electrode surface. The present results are in agreement with those corresponding to the *her*, but a decrease in the maximum current density of the *hor* was not observed, even at high θ_{Bi} values. This different behavior could be due to differences in the nature of Pt substrate, electrolyte solution, and experimental conditions.[9] Therefore, it can be concluded that the interpretation of the present results is consistent with the existence of two types of surface sites. One of them, with lower adsorption energy, is the site involved in the HER (H_{OPD}), while the other, with greater values of the adsorption energy, corresponds to the Bi_{ad} and H_{UPD} sites. This interpretation is also in agreement with the role assigned to the H_{OPD} and H_{UPD} in the kinetic analysis of the HER already proposed.[19,30]

Activated dependence $j(\eta,\theta_{Bi})$.— In order to complete the description of the kinetics of the HER in the presence of bismuth adatoms, the dependences $j(\eta)$ at different θ_{Bi} free of diffusion effects were simulated. Figure 6 shows that, in the anodic region ($0.1 < \eta/V < 0.4$), a limiting kinetic current density significantly greater than that of diffusion nature is clearly defined (Fig. 4). No Tafel domain can be distinguished in the analyzed overpotentials region, as a continuous curvature associated with the variation of the H_{OPD} surface coverage can be seen. It can also be observed from the comparison of Fig. 4 and 6 that in the cathodic region the diffusion effect is still significant.

Finally, the effect of Bi_{ad} on the HER depends strongly on overpotential. Thus, there is a decrease in electrocatalytic activity of the *her* due to the effect of bismuth on the interaction parameter. As the cathodic overpotential is increased, $\theta(\eta)$ increases, the average distance between H_{OPD} atoms decreases, and consequently the interaction effect increases. Therefore, at constant η, $\theta(\eta)$ decreases as θ_{Bi} increases. However, the increase of θ_{Bi} produces only a slight effect on the electrocatalytic activity of the *hor* at $\eta < 0.075$ V, but it is negligible at higher overpotentials. This behavior can be understood if it is taken into account that $\theta(\eta)$ is low at anodic overpotentials.

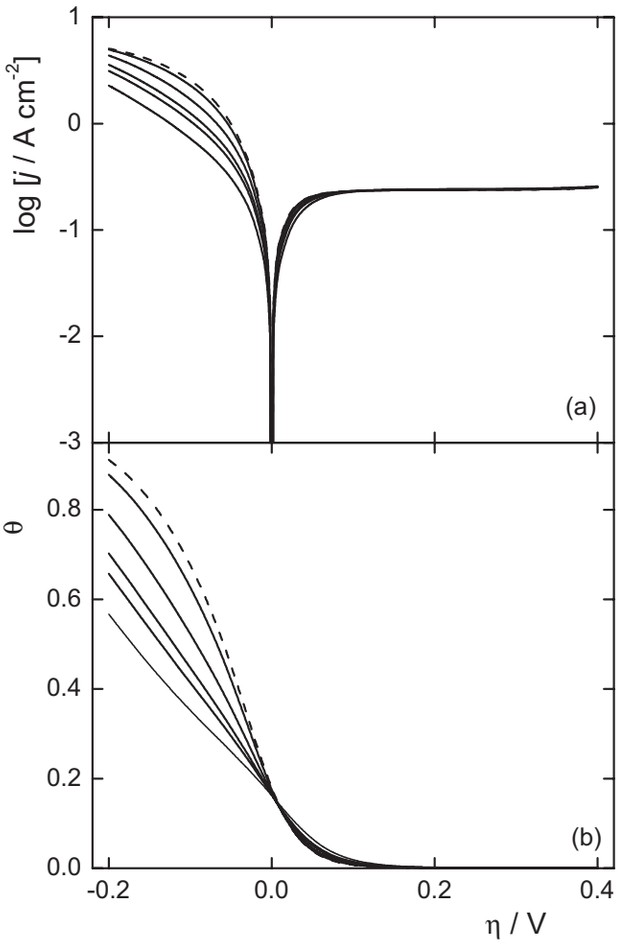

Figure 6. Simulated dependences at different Bi coverages ($0.07 \leq \theta_{Bi} \leq 0.73$) with kinetic parameters from Table I in activated conditions ($j_L \rightarrow \infty$): (a) $\log j$ vs η and (b) θ vs η. Dashed line: Pt electrode.

Conclusions

The experimental determination of the dependences $j(\eta)$ of the HER on a rotating polycrystalline platinum disk with different surface coverage of bismuth atoms was carried out. The results obtained indicate that the sites involved in the Bi adsorption are those corresponding to the adsorption of the H_{UPD} and therefore are different from the sites where the reaction intermediate is adsorbed. The effect of the metallic adatoms on the HER in the whole range of overpotentials was interpreted on the basis of a mixed-control kinetic treatment and a Frumkin-type adsorption for the reaction intermediate. It has been concluded that the decrease in the electrocatalytic activity for the HER is due to the influence of bismuth adatoms on the interaction between the adsorbed atoms of the reaction intermediate.

Acknowledgments

This work was supported by ANPCyT (PICT 14-25587), Conicet (PIP 5645), and UNL (CAI+D 2005-7-41).

Universidad Nacional del Litoral assisted in meeting the publication costs of this article.

References

1. M. Enyo, *Electrochim. Acta*, **18**, 155 (1973).
2. M. Enyo, *J. Res. Inst. Catal. Hokkaido Univ.*, **25**, 17 (1977).
3. J. O'M. Bockris, J. L. Carabajal, B. R. Scharifker, and K. Chandraskaran, *J. Electrochem. Soc.*, **134**, 1957 (1987).
4. M. Elani and B. E. Conway, *J. Appl. Electrochem.*, **17**, 1002 (1987).

5. L. Bai, *J. Electroanal. Chem.*, **355**, 37 (1993).
6. J. Perez, E. Gonzalez, and H. Villullas, *J. Phys. Chem. B*, **102**, 10931 (1998).
7. M. R. Gennero de Chialvo, and A. C. Chialvo, *J. Electroanal. Chem.*, **448**, 87 (1998).
8. D. A. Herrington and B. E. Conway, *Electrochim. Acta*, **32**, 1703 (1987).
9. L. Bai, D. A. Herrington, and B. E. Conway, *Electrochim. Acta*, **32**, 1713 (1987).
10. J. Barber, S. Morin, and B. E. Conway, *J. Electroanal. Chem.*, **446**, 125 (1998).
11. S. Lubetkin, *Electrochim. Acta*, **48**, 357 (2002).
12. P. Delahay, *Double Layer and Electrode Kinetics*, p. 171, John Wiley & Sons, New York (1965).
13. K. J. Vetter, *Electrochemical Kinetics: Theoretical and Experimental Aspects*, Academic Press, New York (1967).
14. J. A. Harrison and Z. A. Khan, *J. Electroanal. Chem. Interfacial Electrochem.*, **30**, 327 (1971).
15. N. M. Markovic, B. Grur, and P. N. Ross, Jr., *J. Phys. Chem. B*, **101**, 5405 (1997).
16. J. X. Wang, S. R. Brankovic, Y. Zhu, J. C. Hanson, and R. R. Adzic, *J. Electrochem. Soc.*, **150**, A1108 (2003).
17. M. S. Rau, P. M. Quaino, M. R. Gennero de Chialvo, and A. C. Chialvo, *Electrochem. Commun.*, **10**, 208 (2008).
18. M. R. Gennero de Chialvo and A. C. Chialvo, *Phys. Chem. Chem. Phys.*, **6**, 4409 (2004).
19. P. M. Quaino, M. R. Gennero de Chialvo, and A. C. Chialvo, *Phys. Chem. Chem. Phys.*, **6**, 4450 (2004).
20. J. X. Wang, T. E. Springer, and R. R. Adzic, *J. Electrochem. Soc.*, **153**, A1732 (2006).
21. P. M. Quaino, J. L. Fernández, M. R. Gennero de Chialvo, and A. C. Chialvo, *J. Mol. Catal. A: Chem.*, **252**, 156 (2006).
22. K. Kunimatsu, T. Senzaki, G. Samjeske, M. Tsushima, and M. Osawa, *Electrochim. Acta*, **52**, 451 (2007).
23. K. Kunimatsu, T. Senzaki, M. Tsushima, and M. Osawa, *Chem. Phys. Lett.*, **401**, 45 (2005).
24. N. Nambu, F. Kitamura, T. Ohsaka, and K. Tokuda, *J. Electroanal. Chem.*, **485**, 128 (2000).
25. R. Gomez, A. Fernandez-Vega, J. M. Feliu, and A. Aldaz, *J. Phys. Chem.*, **97**, 4769 (1993).
26. R. Gomez, J. M. Feliu, and M. Aldaz, *Electrochim. Acta*, **42**, 1675 (1997).
27. T. J. Schmidt, B. N. Grgur, R. J. Behm, N. M. Markovic, and P. N. Ross, Jr., *Phys. Chem. Chem. Phys.*, **2**, 4379 (2000).
28. S. Motoo and T. Okada, *J. Electroanal. Chem. Interfacial Electrochem.*, **157**, 139 (1983).
29. A. C. Chialvo, W. E. Triaca, and A. J. Arvia, *J. Electroanal. Chem. Interfacial Electrochem.*, **146**, 93 (1983).
30. P. M. Quaino, M. R. Gennero de Chialvo, and A. C. Chialvo, *Electrochim. Acta*, **52**, 7396 (2007).
31. S. Sun, S. Chen, N. Li, B. Chen, and F. Xu, *Colloids Surf., A*, **134**, 207 (1998).
32. S. Daniele and S. Bergamin, *Electrochem. Commun.*, **9**, 1388 (2007).
33. R. J. Nichols and A. Bewick, *J. Electroanal. Chem. Interfacial Electrochem.*, **243**, 451 (1988).
34. S. Trasatti, *J. Electroanal. Chem. Interfacial Electrochem.*, **39**, 163 (1972).
35. V. B. Chernogorenko and K. A. Lynchak, *Sov. Powder Metall. Met. Ceram*, **12**, 360 (1973).
36. S. Shibata, *Bull. Chem. Soc. Jpn.*, **36**, 53 (1963).